

Kondo engineering : from single Kondo impurity to the Kondo lattice

J. Flouquet, A. Barla, R. Boursier, J. Derr, and G. Knebel

CEA-SPSMS, 17 rue des Martyrs, 38054 Grenoble Cedex 9, France

In the first step, experiments on a single cerium or ytterbium Kondo impurity reveal the importance of the Kondo temperature by comparison to other type of couplings like the hyperfine interaction, the crystal field and the intersite coupling. The extension to a lattice is discussed. Emphasis is given on the fact that the occupation number n_f of the trivalent configuration may be the implicit key variable even for the Kondo lattice. Three (P, H, T) phase diagrams are discussed: CeRu₂Si₂, CeRhIn₅ and SmS.

KEYWORDS: Kondo effect, Kondo lattice, spin fluctuation, magnetism, superconductivity, pseudogap

In this article we will use the Kondo idea of strong local enhancement of the effective mass m^* of the quasiparticle to understand the new features which appear in a Kondo lattice i.e for a regular array of Kondo paramagnetic centers. Thus an attempt will be given to classify the main parameters of a Kondo impurity and then to schematize the problem by simple relations in order to advance in the experiments on this complex quantum matter which is the Kondo lattice. For simplicity, we restrict the discussion mainly to Ce Kondo centers.

1. Kondo impurity : hierarchy between T_K and other couplings

The new insight into the Kondo effect is that due to the strong coupling with the Fermi sea below some Kondo temperature (T_K) the entropy of a single paramagnetic impurity can collapse at $T \rightarrow 0$ K without further coupling with the other impurities.

One of the important message given by the study of a single Kondo impurity is that the Kondo energy $k_B T_K$ is the key energy in the comparison of the electronic coupling given by the Fermi sea with other sources of interactions like the electronuclear hyperfine coupling A^1 or the crystal field effect C_{CF} .² If $k_B T_K \leq A$ or C_{CF} , the angular momentum J of the Kondo paramagnetic center will feel these inner structures, and only after the selection of a reduced effective spin, the Kondo effect will act and governs the low temperature properties.

A nice case is the hyperfine coupling between the electronic effective spin J and its nuclear spin I submitted to the combined effect of a magnetic field (H) and the Kondo exchange term (Γ) between J and s the spin of the conduction electron according to the hamiltonian

$$H = A\vec{I} \cdot \vec{J} + g_J \mu_B \vec{H} \cdot \vec{J} + g_n \mu_n \vec{H} \cdot \vec{I} - 2\Gamma \vec{J} \cdot \vec{s}$$

This situation was extensively studied by the nuclear orientation method on highly diluted radioactive nuclei. So far $k_B T_K < A$, in a first step I and J are coupled exactly like in atomic

physics. Then the Kondo effect will occur on the selected fundamental state $F = I - J$ or $I + J$ depending the sign of A . When $k_B T_K \geq A$, the behavior of electronic spin will be first governed by the Kondo effect leading in magnetic field to an average value $\langle J_z \rangle$ and thus an effective hyperfine field H_{eff} on the nuclei proportional to the magnetization. This idea is clearly demonstrated in nuclear orientation experiments realized notably on **AuCe** or **LaCe** alloys.³ At zero pressure (P), it was found for **Au**¹³⁷Ce that the electronic spin is mainly coupled to the nuclear spin without any sensibility to any Kondo mechanism (i.e T_K may be lower than mK) why already in **LaCe** a large reduction of H_{eff} is observed by comparison to a free electronuclear motion ($k_B T_K \sim A$). Furthermore, here the measurements under pressure (see figure 1)⁴ point out an increase of T_K by a factor 5 from 120 mK at 0.2 GPa to 600 mK at 1 GPa. The high degree of localisation of the $4f$ electron on the $4f$ shell (occupation number n_f) is also nicely proved by the weak variation of the saturated value.

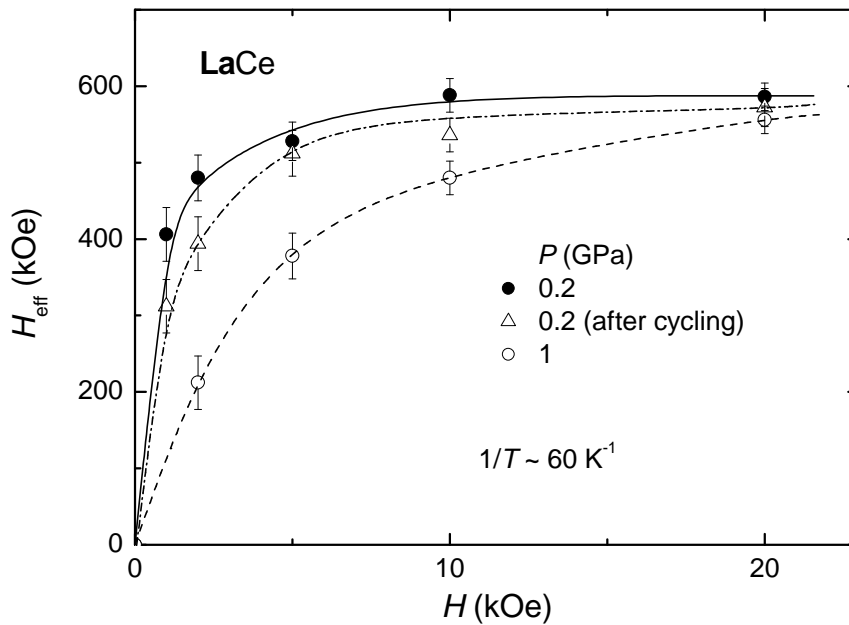


Fig. 1. Nuclear orientation data for **LaCe** at 0.2 and 1 GPa. The solid and dash dotted curves were taken at 0.2 GPa before and after cycling to 1 GPa respectively (after Benoit *et al.*).⁴

An illustration of the interplay between the Kondo effect and the hyperfine coupling was given by the study of the resistivity of **AuYb** realized with different isotopes and thus different hyperfine couplings.⁵ Hyperfine measurements either by nuclear orientation⁶ or Mössbauer effect⁷ push the limit of T_K below the millikelvin range. The element Yb has a number of stable radio-isotopes ; ¹⁷¹Yb and ¹⁷³ have nuclear moments with opposite spin. By choosing the ¹⁷¹Yb isotope, with spin $I = 1/2$, the positive sign of A leads to a zero angular momentum $F = I - J = 0$. Resistivity measurements on figure 2 show the breakdown of the Kondo

scattering for Au^{171}Yb by comparison to the case of Au^{174}Yb (even nuclei with no nuclear moment).

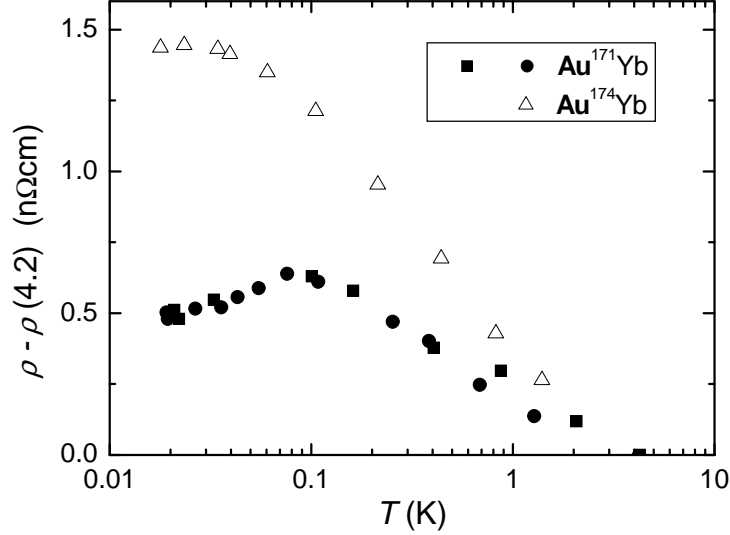


Fig. 2. The square and triangle points describe the Au^{171}Yb resistivity of a 415 ppm alloy, the circle the Au^{174}Yb resistivity of a 396 ppm alloy. The residual logarithmic slope of Au^{171}Yb reflects only the presence of parasitic 5 ppm impurities of ion. The important feature is for Au^{171}Yb , the maximum in the Kondo scattering coincides with the temperature where the singlet electron nuclear state becomes isolated from the triplet excited level (after Hebral *et al.*).⁵

A highly discussed problem is the interplay between $k_B T_K$ and C_{CF} . Experiments notably on Al_2LaCe (see^{2,8} have shown also that provides $k_B T_K \leq C_{CF}$, the Kondo effect at low temperature is realized on the doublet ground state Γ_7 for this cubic material. Under pressure, as we will see later, the Kondo temperature will increase strongly while the crystal field splitting has a smooth pressure variation. The recovery of the full degeneracy under pressure at a pressure P_V is an important issue in the change of a single Kondo behavior but also in the properties of the Kondo lattice.

When the impurity cannot be considered as isolated among the Fermi sea, one must discuss the interplay between the Kondo energy and the intersite coupling E_{ij} . For an effective spin equal to 1/2 i.e for a high degree of the 4f localisation ($n_f \sim 1$), E_{ij} can be mediated by the well known Ruderman, Kittel, Kasuya, Yoshida interaction (RKKY) carried out by the light electron. As a function of Γ and $N(E_F)$ the density of states of the light electron, $k_B T_K$ and E_{ij} can be written⁹ as

$$E_{ij} = \Gamma^2 N(E_F)$$

$$k_B T_K \sim \frac{1}{N(E_F)} \exp\left(-\frac{1}{\Gamma N(E_F)}\right) \quad (1)$$

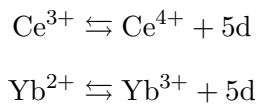
with $\Gamma N(E_F) = \Delta/E_0$ and $k_B T_F = N(E_F)^{-1}$. Δ and E_0 correspond respectively to the line width and position of the virtual $4f$ bound state. These two terms fix n_f . When $k_B T_K \geq E_{ij}$ at a critical pressure P_C , the long range magnetism will collapse according to the popular Doniach scheme.¹⁰ However, the effects in the Kondo lattice may be more subtle, when $k_B T_K$ crosses C_{CF} at P_V , E_{ij} will drop by one order of magnitude.¹¹ Thus P_C can never exceed P_V . Of course, now, the electronic conduction bath is not infinite by respect to the number of cerium sites.

2. From the impurity to the lattice

Three different views can be taken for the collapse of long range magnetism : (1) the previous Doniach scheme,¹⁰ (2) the generalisation of the spin fluctuation theory successfully applied for 3d itinerant magnetism,¹² (3) a push pull mechanism between magnetic and electronic instability strongly related with a change in the occupation number. In the case (1), the Fermi surface is basically assumed to be that given under the assumption of a localized $4f$ electron. In case (2), the $4f$ electron is considered to be already itinerant at a pressure $P_{KL} \leq P_C$. However, in case (3), the quantum effects are furtive with the interferences between spin dynamics, charge motions and their localization.

If the collapse of long range magnetism is via a second order phase transition, one may expect a divergence of the magnetic coherence length ξ_m at P_C coupled with a collapse of a characteristic temperature. In spin fluctuation theory, the corresponding temperature T_{sf} vanishes as $(P - P_C)^\alpha$ with $\alpha = 1$ or $3/2$ for antiferromagnetism or ferromagnetism.¹² If the hidden parameter is the occupation number, one may expect a tiny discontinuity in volume and thus a first order transition with the consequence of finite value of ξ_m and related low Kondo lattice energy T_{KL} .

Figure 3 mimics the situation of Ce^{3+} and Yb^{3+} which corresponds to the trivalent configuration $4f^1$ and $4f^{13}$. The Kondo phenomena is linked with the release of $1 - n_f$ electron from Ce^{3+} or the addition of $1 - n_f$ electron to Yb^{3+} according to the scheme:



For a single impurity, the expression of T_K as a function of the occupation number is given by⁹

$$k_B T_K \sim \frac{1 - n_f}{n_f} \Delta \quad (2)$$

of course T_K depends as n_f of the value of E_0 and Δ (the degeneracy factor N_f has been dropped). In a lattice, there will be a feedback between the Kondo effect on a given site and

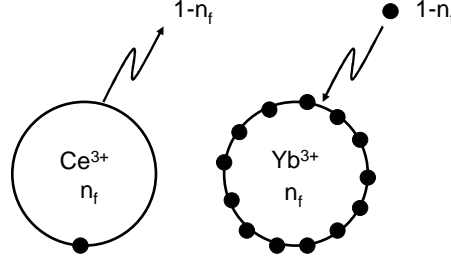


Fig. 3. It is the tiny departure from $n_f = 1$ by the release of $(1 - n_f)$ $4f$ electrons for the trivalent Ce impurity or the absorption of $1 - n_f$ electrons for Yb ion which leads to the Kondo effect.

the Fermi sea. That pushes to propose for the lattice a simple form for T_{KL}^{3+} equal to :

$$T_{KL}^{3+} = (1 - n_f)T_F$$

with $T_F \sim D(n_F)$ a typical electronic bandwidth. T_{KL}^{3+} is attributed to the $3+$ configuration (Ce^{3+} or Yb^{3+}) during its lifetime. (The missing factor n_f in formula 2 will be recovered as the average susceptibility will vary as $n_f \chi_{3+} \sim T_{KL}^{-1} n_f$.)

Looking only to the low carrier doping (i.e neglecting the Brillouin zone). The corresponding relation for T_{KL} for Ce^{3+} and Yb^{3+} configuration will be:

$$k_B T_{KL}(Ce^{3+}) = (1 - n_f)^{5/3} D_0 \quad (3)$$

$$k_B T_{KL}(Yb^{3+}) = (1 - n_f) n_f^{2/3} D_0 \quad (4)$$

where D_0 is the $5d$ bandwidth and independent of n_f . A sound discussion on the relation between T_{KL} , n_f and n_c the extra conduction number in the lattice can be found in Trees *et al.*,¹³ and Ikeda and Miyake *et al.*¹⁴ In this crude model, the striking point is that the dependence T_{KL} for the Ce^{3+} configuration will increase continuously as n_f decreases. For the Yb^{3+} one, as the original free $5d$ electron becomes absorbed in the $4f^{14}$ configuration, T_{KL} will go through a maximum. Thus slow relaxing Yb^{3+} (but also Sm^{3+}) moments characteristic of the trivalent configuration can survive even for a rather weak occupation number ($n_f \sim 2.7$). We want to point out, that one can expect drastic differences between Ce and Yb (or Sm) compounds in the magnetic properties near P_C . Furthermore, the underlining idea is that the effective mass m^* will be finite even at P_C and is basically determined by T_K . The non-divergence of m^* appears clearly in the superconducting phase coupled with the collapse of the antiferromagnetic ordering at P_c . Rather moderate values of the strong coupling parameter is required for a good fit of the upper critical field.

but the associated coherence length ℓ_{LK} associated with T_{KL} and m^* can strongly increase near P_C . Furthermore, the $5d$ electrons may react to the $4f$ correlations. So D may depend on a less trivial form on n_f . For example, $D(n_f)$ may reach a high value for $n_f \rightarrow 1$ and a weak one for $n_f \leq 2.8$. An illustration will be given below with the gold phase of SmS where obviously at small enough pressures ($P < P_\Delta$ see later) the $5d$ electron prefers to be trapped

around the Sm centers. The relation of the pseudogap shape of D with n_f is a central issue in strongly correlated electronic systems and will not be discussed here.

The key problem is to derive a characteristic temperature for the lattice. It is amazing that in the limit of low carrier density it was proposed that T_{KL} varies as $n^{1/3}$.¹⁶ With the previous relation 4, this prediction is recovered in the Yb case remaining that $T_{KL} = T_{KL}(\text{Yb}^{3+})/n_f$. Another suggestion was that T_{KL} goes like T_K^2 ,¹⁷ an expression not so far to the initial $T_K^{5/3}$ law proposed for the Ce case. An appealing possibility is that as the effective mass increases, its coherent circulation over the Kondo loop increases. If ℓ_{KL} is proportional to m^* , the heavy particle of mass m^* will travel through the full Kondo loop after a time $\tau_{KL} \sim (m^*)^2$. Of course the great novelty is that the situation is different from that found in normal rare earth intermetallic compound where the information is carried by light particles with mass near the bare electronic mass m_0 over a small atomic distance a_0 leading to a fast response $\tau_0 \sim m_0 a_0$. This slow motion over large distances may lead to unusual time and space response of the quasiparticle.

3. Pressure effects

Discussing the pressure variation of T_K for a single impurity requires to know the relative pressure variation of Δ and E_0 . The expression for Δ as a function of the hybridization term v_{dk} between the f and light electron is :

$$\Delta = \pi v_{dk}^2 N(E_F)$$

The pressure increase of Δ is related to the increase of the bandwidth of the Fermi sea. It is wellknown for normal metal that the volume variation of T_F is governed by the increase of the atomic density leading to a Grüneisen parameter $-\frac{\partial \log T_F}{\partial \log V} = \Omega_F = +2/3$. If we assume $v_{dk} \sim N(E_F)^{-1}$ one recover the formula suggested for the Kondo lattice as $\Delta \sim T_F$. The high sensitivity of the cerium impurity to P can be easily understood (assuming E_0 fixed) by the weakness of $\Delta/T_F \sim 10^{-2}$ in comparison to $E_0/T_F \sim 0.2$. After equation 1, with T_K equal to:

$$T_K = T_F \exp\left(-\frac{E_0}{2 \cdot 10^{-2} T_F}\right)$$

the Grüneisen parameter of T_K becomes

$$\Omega_{T_K} = \Omega_{T_F} \left(1 + \frac{50E_0}{T_F}\right) \sim 10\Omega_{T_F}.$$

If E_0 is reduced of course there will be an extrasource of an amplification.

Another evaluation of Ω_{T_K} can be made via the relation 2. Of course T_K depends on two parameters, n_f and Δ but assuming $\Delta = T_F$, the main source of variation of T_K arises through that of n_f :

$$\frac{\partial T_K}{T_K} \sim \frac{1}{(1 - n_f)} \frac{\partial n_f}{n_f}$$

with the crude estimate that n_f varies linearly with the volume according to Vegard's law :

$$n_f = \frac{V - V_{4+}}{V_{3+} - V_{4+}}$$

V_{3+} and V_{4+} being the volume attribute to the 3+ and 4+ configuration. One gets

$$\Omega_{T_K} \sim \frac{1}{(1 - n_f)} \frac{V_{3+}}{(V_{3+} - V_{4+})} \text{ for } n_f \rightarrow 1;$$

For $V_{3+} - V_{4+} = 0.5V_{3+}$ (the 4f configuration is in fact never reached for the cerium case) , the Grüneisen parameter of T_K will be $\Omega_{T_K} \sim 2(1 - n_f)^{-1}$. For cerium heavy fermion compounds $n_f \gtrsim 0.9$, thus $\Omega_{T_K} \gtrsim 20$.

Basically, Ω_{T_K} and m_K^* , the local effective mass due to the Kondo effect $m_K^* \sim \frac{1}{T_K}$ scale each other. As pointed out,²¹ a constant ratio Ω/m_K^* will imply a logarithmic dependence of the interaction responsible for the dressing of the quasiparticle. Recent developments in high energy spectroscopy of Kondo systems have lead to a direct charge visualization of the Kondo resonance for cerium intermetallic compounds. However, the extrapolation to the single impurity parameter is not straightforward (see Malterre et al.¹⁸). Let us stress here that qualitatively the results obtained on Ce compounds agree with our previous statements. The situation is far less clear for the the Yb systems. It was already underlined that the differences reflect a smaller interconfiguration energy in the Yb case than in the Ce one. For Ce, the $4f^0$ and the $4f^1$ configurations are separated by 2 eV. For Yb, the separation can be less than 100 meV.¹⁸

In temperature, the experimental Grüneisen parameter defined as the ratio of the thermal expansion $\alpha = -\frac{1}{V} \frac{\partial V}{\partial T}$ by the specific heat C (normalized by the molar volume V and the compressibility κ) is a simple powerful tool to test if the free energy F depends only on one parameter (T^* , here T_K for a single impurity) as if :

$$F = T\Phi(T/T^*)$$

$$\Omega(T) = \Omega_0 = \text{constant}$$

$$\Omega(T) = -\frac{\partial \log T^*}{\partial \log V} = \frac{\alpha V}{C \kappa}$$

Typical values for Kondo impurity are around 50. The remarks of large Grüneisen parameters for heavy fermion compounds were made in.,^{19,20} The thermal expansion is huge as it goes then as $(m^*)^2$. If m^* is three order larger than the bare electronic mass, the corresponding electronic thermal expansion is six times higher than the usual electronic one. That leads us to suspect that the density fluctuations are crucial in the heavy fermion problems and notably in Cooper pair pairing.

When we will consider the lattice, the study of the ratio α/C in temperature is a sound cheap way to test if competing interactions occur. The slow recovery of a constant $\Omega(T)$ is the indication to the "tenuous" entrance in a Fermi liquid regime. In spin fluctuation theory, the effective mass increases at P_c but stays finite while $\Omega^*(P_c)$ diverges.^{12,22}

4. CeRu₂Si₂ : an example of paramagnetic Kondo lattice

The tetragonal compound CeRu₂Si₂ at zero pressure realized ideal conditions for the understanding of a high correlated Kondo lattice : $P_C \sim -0.3$ GPa will be located few kbar below $P = 0$, furthermore P_V is near 4 GPa.²³ So a large pressure range exists for a careful study of a spin 1/2 Kondo lattice. The tuning below P_C can be even achieved by expanding the lattice with lanthanum²⁴ or germanium substitution. In the serie Ce_{1-x}La_xRu₂Si₂, antiferromagnetism (AF) is only detected for $x \geq 0.075$. The figure 4 represents the specific heat data for well ordered compounds $x > 0.075$ and a paramagnetic ground state $x = 0.075$. In the $x = 0.05$ paramagnetic case, the slow increase of C/T on cooling reflects the so called large crossover non Fermi liquid regime. The usual Fermi liquid dependence of C/T for a nearly antiferromagnet

$$\frac{C}{T} = \gamma + \beta T^2$$

will only by recovered at very low temperature. By contrast to the single Kondo effect governed

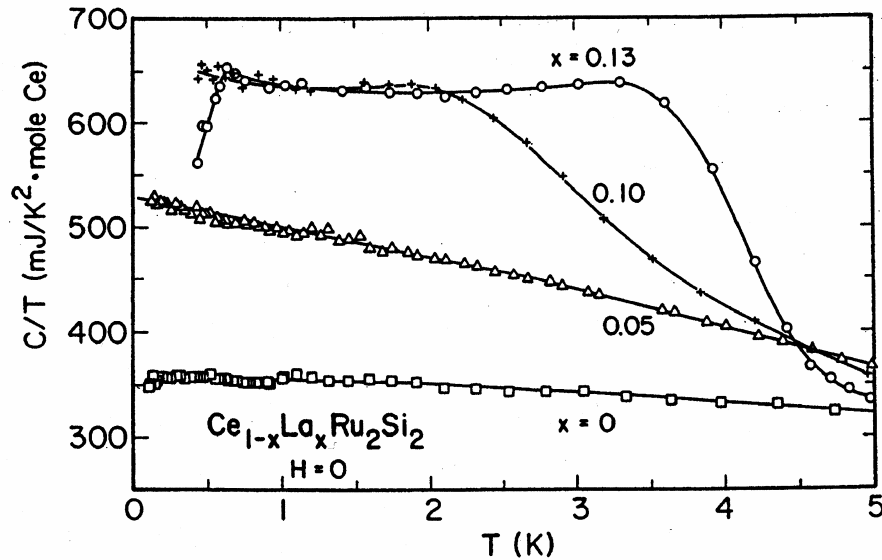


Fig. 4. Specific heat of Ce_{1-x}La_xRu₂Si₂ on the both side of the critical concentration $x_c = 0.075$. For $x = 0.13$, antiferromagnetism is observed. For $x = 0.05$, paramagnetism exists down to 0K.

by a single parameter T_K , over a large temperature range $T \lesssim T_K$, the slow development of the coherence between the spin and charge motion is pointed out in the temperature evolution of $\Omega^*(T)$ ²⁵ which reaches a constant only at very low temperature (fig. 5). The complexity in the continuous process for the formation of the heavy quasiparticle on cooling emerges in the different macroscopic experiments. Large differences appear in the characteristic temperature as $T_{-,+} \sim 60$ K the temperature where the initial magnetoresistance goes from negative to

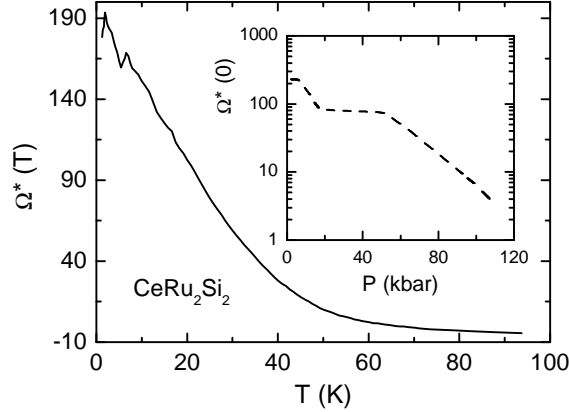


Fig. 5. Temperature variation of the Grüneisen parameter measured by the normalized ratio of the thermal expansion by the specific heat. In inset, pressure variation of the Grüneisen parameter extrapolated to $T = 0$ K.

positive, $T_C^M \sim 12$ K, $T_\chi^M = 10$ K, $T_\alpha^M = 8.7$ K the temperature of the maxima in specific heat, susceptibility and thermal expansion, $T_Q \sim 0.5$ K where the thermoelectric power Q reaches its T linearity and $T_A = 0.3$ K where the Fermi liquid inelastic AT^2 term is observed in resistivity.¹⁵

The excellent quality of large crystal have allowed two important microscopic experiments. Inelastic neutron measurements show clearly that antiferromagnetic correlations set in at $T_{-,+}$; even at $T \rightarrow 0$ K, the coherence length is restricted to few atomic distances.¹⁵ De Haas van Alphen experiments needs the itineracy of the f electrons to be explained selfconsistently with band calculations at least $P_{KL} \leq P_V$. An effective mass up to 120 m_0 has been detected.^{26,27} Applying pressure in CeRu_2Si_2 leads to a strong decrease of m^* ($\Omega^*(P=0) \sim 190$).²⁸ The derivation of the pressure variation of the Grüneisen parameter shows that Ω^* reaches another plateau at $P_V \sim 4$ GPa with $\Omega^*(0) = 80$.

An external magnetic field can modify the nature of the magnetic interactions. The metamagnetic field H_C characteristic of the AF (H, T) phase diagram ends up at a critical point at P_C .²⁹ For $P \geq P_C$, only a well defined crossover at H_M will occur between a low field state dominated by AF correlations ($H \leq H_M$) and a high field phase ($H \geq H_M$) dominated by ferromagnetic (F) coupling and the progressing alignment of the cerium magnetization. That leads to drastic changes in some characteristic temperatures as T_α .²⁴ Figure 6 represents the deep minima reached by T_α at H_M : $T_\alpha(H_M) \sim 0.3$ K i.e roughly the value of T_A at $H = 0$. The switch from AF to F correlations,^{15, 30,31} have been nicely observed in neutron scattering experiments as well as associated drastic changes of the Fermi surface through H_M .^{26,27}

It is worthwhile to underline that P and H are generally different. Under pressure here, the dominant AF correlations are preserved, but slowly mollified on approaching P_V . So the phenomena at P_C for $H < H_M$ can be ranked as AF quantum critical behavior. In H there

is a switch in the nature of the correlations at H_M which emerges from a critical end field $H_c(P_c)$. However the change from AF to F interactions is governed by the H shift of the Fermi level inside the pseudogap structure created in this Kondo lattice.³³ Thus the quasi divergence of $\Omega^*(H, P = 0)$ occurs at H_M .¹⁵ If H_c will continuously collapse with T_N as $P \rightarrow P_c$, the magnetic field opens the possibility to tune at low magnetic fields through P_c .³² A rich variety of (H, P, T) puzzles with new figures can be drawn with the interplay of the crossover phase diagram of figure 6 and classical phase diagrams for magnetism and superconductivity

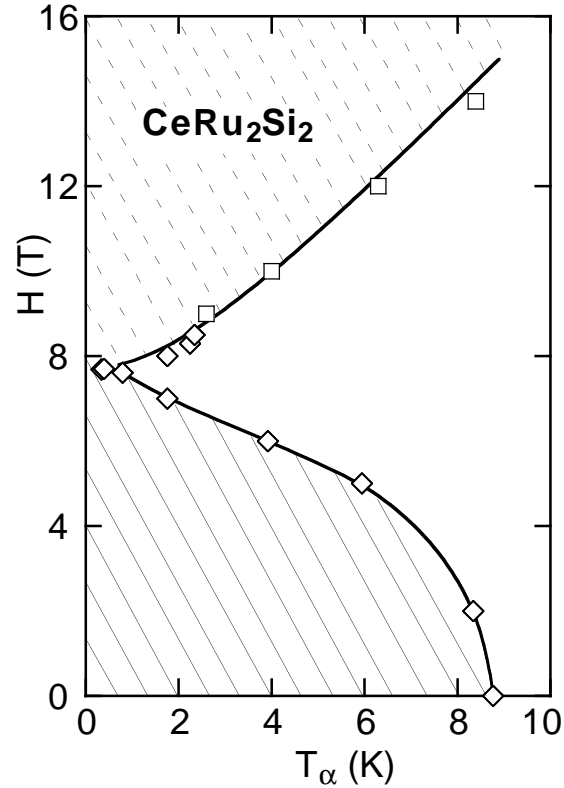


Fig. 6. Field dependence of the temperature of the optimum of the thermal expansion measured at different field $\alpha_H(T)$. The full line describes the low field paramagnetic phase dominated by AF correlations, the dashed lines the high field phase dominated by a F coupling.

Towards these clear facts, the paramagnetic phase of CeRu_2Si_2 may be the matter of new motions (magnetic current) as a tiny magnetism (sublattice magnetization near $10^{-3}\mu_B$) has been detected around $T \sim 2\text{K}$ ³⁴ with an associated signature in the thermoelectric power.³⁵ An appealing possibility of this furtive magnetism is that it will be a macroscopic consequence of the circulation of the quasiparticle along their special Kondo lattice loop. Another open question is the validity of the concept of a second order phase transition. New experiments on $\text{Ce}_{0.925}\text{La}_{0.075}\text{Ru}_2\text{Si}_2$, which is located at $x = x_c$, shows clearly that the characteristic energy does not collapse³⁶ at x_c . The dogma of a second order quantum critical point may be revisited.

The interesting perspective is that the magnetic instability is associated with a change in the localization of the particle (i.e in a discontinuity of n_f). Indeed for CeIn_3 ,³⁷ CePd_2Si_2 ³⁸ and CeRh_2Si_2 ,³⁹ $P_C = P_V$ and first order transitions at P_C are observed^{37,39} or strongly suspected.³⁸ Of course, the transition may be weakly first order as large fluctuations are generally observed in the specific heat. It is worthwhile to compare with the first order liquid-solid transition of ^3He where on the melting curve at $P \sim 34$ bar the volume discontinuity is near 5%. For heavy fermions, P_C is often around 3 GPa, i.e. three orders of magnitude larger than in ^3He . Thus a volume discontinuity of 5×10^{-5} will give a comparable mechanical work ($P\Delta V$) than in ^3He on its melting curve. Tiny first order transitions may correspond to a 10^{-7} or less effect on the volume contraction.

To go back on the hyperfine coupling, it is worthwhile to point out that for Ce only an even stable isotope exists. There is no hyperfine coupling. However for natural Yb, four isotopes exist two even ($I = 0$) ^{172}Yb and ^{174}Yb but two odd, ^{171}Yb ($I = 1/2$) and ^{173}Yb ($I = 5/2$). If $T_{KL} \leq A$, the full electronuclear dynamic must be considered. Even, an unusual magnetic ordering may be boosted by the nuclear spin. This may lead to new features for the Yb compounds in comparison to the cerium heavy fermion compounds. Surprisingly for YbRh_2Si_2 even with a very low Néel temperature $T_N \sim 70$ mK and tiny ordered moments (see³¹), a very nice specific heat anomaly occurs while in Ce Kondo lattice, tiny calorimetric signature is only visible.¹⁵ Recent experiments on YbRh_2Si_2 with the ^{174}Yb isotope shows the persistence of magnetic ordering.⁴⁰ The different behavior between the CeRu_2Si_2 serie and YbRh_2Si_2 may be due to $4f$ - $5d$ correlations not included in the usual Kondo approaches.

5. Magnetism and superconductivity

In heavy fermion compounds, superconductivity appears related with magnetic and valence instabilities (P_C and P_V). The P and H tunings of the electronic correlations give unique tools in the interplay between magnetism and superconductivity. Furthermore due to the weakness of the parameters ($T_{KL} \sim 1$ K, $H_M \sim 10$ T) experiments can be realized with small scale equipments. In the previous case of CeRu_2Si_2 , no superconductivity has been detected under pressure. That may emphasize at P_C either the weakness of the pairing mechanism for Ising spin as Ce in CeRu_2Si_2 ¹⁵ or as observed for CeRh_2Si_2 ³⁹ a sharp superconducting domain right at P_C . Around P_V , new careful pressure experiments must be realized to test if another superconducting domain may exist as found for CeCu_2Si_2 ⁴¹ and CeCu_2Ge_2 .⁴²

Recently, careful ac calorimetric experiments⁴³ were done on the new discovered 115 CeRhIn_5 compound.⁴⁴ The great experimental interest of this material is that the optima of their magnetic ordering at T_N and superconductivity at T_C temperatures are comparable and located in a easy range of temperature ($T \sim 2$ K). As shown in figure 6, AF disappears via a first order transition. In good agreement with this statement, AF never succeeds to superconductivity on cooling. Below P_C , the opposite occurs but the superconducting phase

is gapless. Our proposal is that specific heterogeneities occurs when T_N starts to decrease deeply. Here bulk superconductivity and antiferromagnetism may be antagonist.

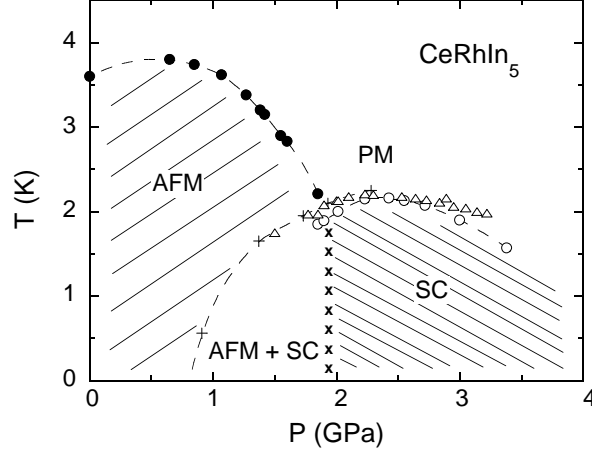
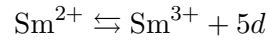


Fig. 7. Phase diagram of CeRhIn₅ as determined by specific heat (● and ○) and susceptibility (△). In addition $T_C(P)$ from resistivity measurements after⁴⁵ (×) marks the first order phase boundary between antiferromagnetism (AF) and superconductivity (SC).

6. Valence, conduction and magnetism : SmS

One of the fascinating facet of the Kondo lattice illustrated in SmS experiments,^{44, 45, 46} is that the physical properties may look that of a specific configuration Sm²⁺ ($J = 0$) or Sm³⁺ ($J = 5/2$) despite the fact the occupation number n_f is far from unity. New results on SmS demonstrate the curious dressing of the heavy electrons. SmS is a key matter as the previous equilibrium:



governs the release of a $5d$ itinerant electron.

In the divalent black (B) phase, Sm²⁺ S²⁻ is an insulating non magnetic as $J = 0$ for the $4f^6$ Sm²⁺ configuration. In the intermediate valent gold (G) phase, the valence v is near 2.7 ($v = 2 + n_f$) right at the first order phase transition at $P_{B-G} \sim 1.2$ GPa ; the high temperature behavior corresponds to the disordered regime of a Kondo lattice but at low temperature up to $P_\Delta \sim 2$ GPa the ground state ends up in a non magnetic insulating phase : D depends on n_f . Above P_Δ for $v \sim 2.8$, SmS is a metal at $T \rightarrow 0$ K ; its metallic behavior is quite analogue to that reported for ordinary heavy fermion compounds.

The simultaneous achievement of a macroscopic ac specific heat measurements⁴⁶ and of a microscopic nuclear forward,^{47,48} scattering experiments (NFS) gives now a complete view of the interplay between valence, electronic conduction and magnetism. Right at P_Δ , evidences were found below NFS for the slow spin motions of a Γ_8 ground state of Sm³⁺ above $T_{NFS} \geq$

T_N .^{46,47} The surprise is that $P_\Delta = P_C$ i.e magnetic ordering occurs far below the pressure P_{3+} where the trivalent state will be reached at $P_{3+} \geq 10$ GPa⁴⁹ (see figure 8).

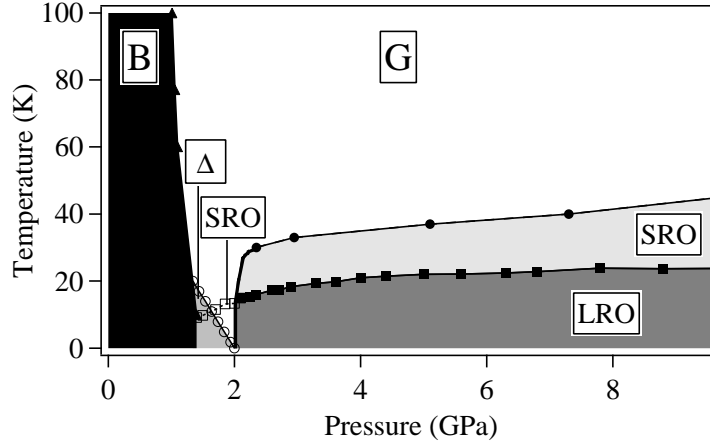


Fig. 8. Phase diagram of SmS in the gold phase. Slow relaxation is observed in NFS experiments at T_{NFS} , ac calorimetric measurements has located the ordering temperature T_N . Short range magnetic correlations persists in the low pressure ($P \leq P_\Delta$) of the gold phase where a gap occurs for the electronic conduction. Above P_V , the ground state is AF and metallic. The trivalent state is reached far above 10 GPa,^{48,49}

An explorer at $T = 0$ K, who can look to changes in volume, conduction and magnetism, will feel large change of volume at P_{B-G} tiny change at $P_\Delta = P_C$. He will detect the concomitant variation of the conduction and the magnetism also at $P_\Delta = P_C$. If he looks carefully in time, he may find evidences of a sloppy matter between P_{B-G} and P_Δ with unusual spin dynamics reminiscent of the Sm^{3+} configuration. At the average below P_Δ no difference seems to occur between the 2+ and 3+ configurations since both present an isotropic paramagnetism with equal sizes for their local susceptibility with either a van Vleck (2+) or a Pauli (3+) origin.

7. Conclusion

The concept of Kondo impurity gives a huge impact in the physics of quantum complex systems. Its extension to Kondo lattice is already successful at least for the experimentalists. With slight modifications (insertion of a pseudogap i.e. strong n_f dependence of D), it appears possible to track the problem of the consistency between spin and charge motion and to follow some routes in the search for new effects and the discovery of new materials. Of course, in materials sciences, the Kondo engineering label covers also the domain of artificial Kondo nanostructures. We can argue of course on the validity of the engineering addenda to Kondo. At least, it reinforces that the fundamental open questions remain. Experimentalists can built or look to new electronic and magnetic architectures or devices. In any case, the common

points are that the initial potential has an atomic origin, the correlation length reaches nanometric size and high purity material with an electronic mean free path above 1000 Å can be achieved. Clean experiments have been already achieved and excellent perspectives exist to go behind the standard accepted concepts to enjoy fancy spin and charge motion and even to open new windows for applications. It may be also worthwhile to mention that the goal to elucidate fundamental problems has boosted the development of new instrumentations which have now wide applications from astrophysics cosmology to nanophysics and material sciences. The Kondo problem was a clear challenge which has required new concepts but also huge progress in the observation of low temperature physics.

JF thanks Profs. J. Friedel, T. Kasuya, K. Miyake, R. Tournier and Drs J.P. Brison, P. Haen and D. Jaccard for stimulating discussions.

References

- 1) J. Flouquet: *Prog. Low. Temp. Physics* VII, eds. (Elsevier, North Holland, 1978).
- 2) B. Cornut and B. Coqblin: *Phys. Rev. B* **5** (1992) 4541.
- 3) J. Flouquet: *Phys. Rev. Lett.* **27** (1971) 515.
- 4) A. Benoit, J. Flouquet, and J. Sanchez: *Phys. Rev. Lett.* **32** (1974) 222.
- 5) B. Hebral, K. Matho, J. M. Mignot, and R. Tournier: *J. Phys. Lett.*; **38** (1977) L347.
- 6) A. Benoit, J. Flouquet and J. Sanchez: *Phys. Rev. B* **1** (1974) 4213.
- 7) F. Gonzalez Jimenez and P. Imbert: *Solid State Commun.* **13** (1973) 85.
- 8) F. Steglich: in *Festkörperproblem* (Advances in Solid State Physics) (Vieweg, Braunschweig, 1977) ed. J. Treusch, Vol XVII, p. 319.
- 9) A.C. Hewson, *The Kondo problem to heavy fermions* (Cambridge University Press, 1992).
- 10) S. Doniach: *Physica B* **91** (1977) 231.
- 11) R. Ramakrishnan: *Valence fluctuations in solid* (North Holland Publishing Company, 1981) eds. L.M. Falikov, W. Hanke and M.B. Maple, Vol 13.
- 12) T. Moriya and Takimoto: *J. Phys. Soc. Jpn.* **64** (1995) 960.
- 13) B.R. Trees, A. J. Fedro, and M. R. Norman: *Phys. Rev. B* **51** (1995) 6167.
- 14) H. Ideka and K. Miyake: *J. Phys. Soc. Jpn.* **66** (1997) 3714.
- 15) J. Flouquet, to be published, *Prog. Low Temp. Phys.*, eds A. Halperin (North Holland) (2004).
- 16) S. Burdin, A. Georges, and D. R. Grempel: *Phys. Rev. Lett.* **85** (2000) 1048.
- 17) P. Nozières: *Eur. J. Phys. B* **6** (1998) 447 .
- 18) D. Malterre, M. Grioni, and Y. Baer: *Advances in Physics* **45** (1996) 299.
- 19) A. Benoit, A. Berton, J. Chaussy, J. Flouquet, J. C. Lasjaunias, J. Odin, J. Pellaue, and J. Peyrard: *Valence fluctuations in solid* (North Holland Publishing Company, 1981) eds. L.M. Falikov, W. Hanke and M.B. Maple, Vol 13.
- 20) R. Takke, M. Nicksch, W. Assmus, B. Lüthi, R. Pott, R. Schefzyk, and D. K. Wohlleben: *Z. Phys. B* **44** (1981) 33.
- 21) D. Jaccard and J. Flouquet: *J. Magn. Magn. Mat.* **47-48** (1985) 45.
- 22) L. Zhu, M. Garst, A. Rosch, and Q. Si: *Phys. Rev. Lett.* **91** (2003) 066404.
- 23) J. Flouquet, P. Haen, S. Raymond, D. Aoki, and G. Knebel: *Physica B* **319** (2002) 251.
- 24) R.A. Fisher, C. Marcenat, N. E. Phillips, P Haen, F. Lappiere, P. Lejay, J. Flouquet and J. Voiron: *J. Low Temp. Phys.* **84** (1991) 49.
- 25) A. Lacerda, A. de Visser, L. Puech, P. Haen, and J. Flouquet: *Phys. Rev. B* **40** (1989) 11429.
- 26) H. Aoki, M. Takashita, S. Uji, T. Terashima, K. Maezawa, R. Settai, Y. Onuki: *Physica B* **206-207** (1995) 26.
- 27) S.R. Julian, F. S. Tautz, G. J. McMullan, and G. G. Lonzarich: *Physica B* **199-200** (1994) 63.
- 28) K. Payer P Haen, J. M. Laurant, J. M. Mignot, and J. Flouquet: *Physica B* **186-188** (1993) 503.
- 29) P. Haen *et al.*: *J. Phys. Soc. Jpn.* **65** (1996) suppl. B, 27 .
- 30) S. Raymond, D. Raoelison, S. Kambe, L. P. Regnault, B. Fak, R. Calemezuk, J. Flouquet, P. Haen, and P. Lejay: *Physica B* **259-261** (1999) 48.
- 31) M. Sato *et al.*: to be published.
- 32) C.V. Custers, P. Gegenwart, H. Wilhelm, K. Neumaier, Y. Tokiwa, O. Trovarelli, C. Geibel, F. Steglich, C. Pepin, and P. Coleman: *Nature (London)* **424** (2003) 524.

- 33) H. Satoh and F.J. Ohkawa: Phys. Rev. B **63** (2001) 184401.
- 34) A. Amato, B. Baines, R. Feyerherm, J. Flouquet, F. N. Gygax, P. Lejay, A. Schenk, and U. Zimmermann: Physica B **186-188** (1993) 276.
- 35) A. Amato, D. Jaccard, J. Sierro, P. Haen, P. Lejay, and J. Flouquet: J. Low Temp. Phys. **77** (1989) 195.
- 36) W. Knafo, PhD thesis, University Grenoble (2004)
- 37) G. Knebel, D. Braithwaite, P. C. Canfield, G. Lapertot, and J. Flouquet: Phys. Rev. B **65** (2002) 024425.
- 38) A. Demuer, A. T. Holmes, and D. Jaccard: J. Phys. Condens. Matter **14** (2002) L529.
- 39) S. Araki, Nakashima, R. Settai, T. C. Kobayashi, and Y. Onuki: J. Phys. Condens. Matter **14** (2002) 377.
- 40) V. Glazkov and G. Knebel, private communication.
- 41) A.T. Holmes, D. Jaccard, and K. Miyake: Phys. Rev. B **69** (2004) 024508.
- 42) D. Jaccard, K. Behnia, and J. Sierro: Phys. Lett. A **163** (1992) 475.
- 43) G. Knebel et al, to be published (2004).
- 44) J.D. Thompson, R. Movshovich, Z. Fisk, F. Bouquet, N. J. Curro, R. A. Fisher, P. C. Hammel, H. Hegger, M. F. Hundley, M. Jaime, P. G. Pagliuso, C. Petrovic, N. E. Phillips, and J. L. Sarrao: J. Magn. Magn. Mat. **226-230** (2001) 5.
- 45) A. Llobet, J. S. Gardner, E. G. Moshopoulou, J. M. Mignot, M. Nicklas, W. Bao, N. O. Moreno, I. N. Gonscharenko, J. L. Sarrao, and J. D. Thompson: Phys. Rev. B **69** (2004) 024403.
- 46) A. Barla, J. P. Sanchez, Y. Haga, G. Lapertot, B. P. Doyle, O. Leupold, R. Ruffer, M. M. Abd-Elmeguid, R. Lengsdorf, and J. Flouquet: Phys. Rev. Lett. **92** (2004) 066401.
- 47) Y. Haga, A. Barla, J. Derr, B. Salce, G. Lapertot, I. Sheikin, K. Matsubayashi, N. K. Sato, and J. Flouquet, to be published (2004).
- 48) A. Barla, J. P. Sanchez, J. Derr, B. Salce, G. Lapertot, J. Flouquet, B. P. Doyle, O. Leupold, R. Ruffer, M. M. Abd-Elmeguid, and R. Lengsdorf, to be published in J. Phys. Condens. Matter, cond-mat/0406166
- 49) J. Röhrer et al, Valence instabilities, eds. P. Wachter and H. Boppart (Amsterdam, North Holland) p. 215 (1982).
- 50) C. Dallera, E. Annexe, J. P. Rueff, M. Grioni, G. Yanko, L. Braicovich, A. Barla, J. P. Sanchez, R. Gusmeroli, A. Polenzana, L. Degiorgi, and G. Lapertot: to be published in J. Condens. Matter (20)